

Continuous monitoring of bedload discharge in a small, steep sandy channel

Ana Lucía ^{a,b,1}, Alain Recking ^c, José F. Martín-Duque ^{a,1}, Yael Storz-Peretz ^d, Jonathan B. Laronne ^{d,e,*}

^a Department of Geodynamics and Institute of Geosciences (CSIC, UCM), Complutense University of Madrid, Ciudad Universitaria, C/José Antonio Novais No. 2, Madrid E-28040, Spain

^b Faculty of Science and Technology, Free University of Bolzano, Piazza Università, 5, 39100 Bolzano, Italy

^c Irstea 2 rue de la papeterie, BP 76, 38402 Saint Martin d'Hères Cedex 38402, France

^d Department of Geography and Environmental Development, Ben-Gurion University of the Negev, Beer-Sheva 84105, Israel

^e Laboratoire d'Etude des Transferts en Hydrologie et Environnement (LTHE), Université Joseph Fourier, 38041 Grenoble Cedex 09, France

S U M M A R Y

This paper reports on bedload flux and texture monitored in a natural, steep, sandy ephemeral channel draining a small gullied sandy watershed, the Barranca de los Pinos (1.32 ha), Spain. Bedload flux was continuously monitored with two independent Reid-type slot samplers; bedload texture was determined from the sediment collected in the samplers. Channel morphology was surveyed with a high spatial resolution with a Terrestrial Laser Scanner.

The monitored instantaneous bedload fluxes are among the highest measured in natural rivers, characterized by high temporal and spatial variability related to the presence of bedforms, shallow bars and sand sheets, and to the reworking of the dry bed between and at the end of individual flow events. The grain size distribution of the bedload indicates equal mobility; but bedload texture fluctuates, depicting the transport of coarser bar surfaces and of finer-grained anabranch surfaces as well as of the overall bed subsurface.

Keywords:

Bedload flux, Sand-bed channel; Ephemeral stream; Steep stream; Reid-type slot sampler; Braiding

1. Introduction

Bedload transport is a fundamental process shaping stream channels. The interrelationships between water, transport of sediment and bed configuration are complex and the mechanical principles that govern their behavior are not yet adequately explained (Turowski, 2010). Bedload transport is a challenging area of research due to its high temporal and spatial variability (Gomez, 1984), the interaction of different sizes of bed material (Parker, 2008) and the fact that the transport of coarse sediment itself may change channel geometry (Ashmore, 1991). The knowledge of bedload transport mechanisms is of importance, not only academically to better understand the underlying processes and forms, but also to aid managers and engineers in informed and appropriate decision making concerning river and riverine environments (Lancaster and Grant, 2003).

Bedload measurements have been undertaken under a variety of environmental settings. These include river channels with different grain size distributions (sand to boulder beds), bedforms and bed patchiness, gradients and hydrologic regime (perennial to ephemeral). Measuring bedload transport is expensive, time consuming and also dangerous in some settings, hence measurements of bedload are less common than those of suspended sediment (Gray et al., 2010). In flumes, bedload has been monitored under controlled conditions with uniform material (e.g., Meyer-Peter and Müller, 1948) and with mixed size sediment (e.g., Iseya and Ikeda, 1987; Recking et al., 2009). In the field bedload transport is difficult to measure due to the complexity of this phenomenon (Haff, 1996) as it entails high spatial and temporal variability, complex grain size distribution and large sizes, high flow velocities and turbid flow. Moreover it is difficult to determine when and how sediment moves on the bed; also, the flow and bed may be disturbed by deployment of bedload samplers (Holmes, 2010). Three types of devices have been used to measure bedload transport in rivers. The first involves the use of portable samplers, such as the Helley-Smith (Helley and Smith, 1971), Arnhem (Schaank, 1937) or Delft-Nile (Van Rijn and Gaweesh, 1992) and portable traps

* Corresponding author at: Department of Geography and Environmental Development, Ben-Gurion University of the Negev, Beer-Sheva 84105, Israel.

E-mail address: john@bgu.ac.il (J.B. Laronne). ¹ Tel.: +34 913944857; fax: +34 913944845.

(Bunte et al., 2001). Data obtained with these samplers are limited to a single location for a short time interval, but the samplers are movable between sites. The second includes devices that allow the continuous direct measurement of bedload transport at fixed locations, such as the continuous belt slot system at the East Fork River (Leopold and Emmett, 1977), the channel-wide vortex slot (Milhous, 1973), the ultrasonic sensor system developed in Rio Cordon (D'Agostino and Lenzi, 1999) and the Reid-type recording slot sampler (Reid et al., 1980). The latter has been the most widespread method, having been used successfully in permanent and ephemeral gravel bed rivers worldwide (García et al., 2000; Lar-onne et al., 2003).

More recently, surrogate monitoring technologies, such as Acoustic Doppler Current Profilers – ADCPs (Gaeuman and Jacobson, 2006a), geophones (Mizuyama et al., 2010; Rickenmann and Fritsch, 2010) and hydrophones (Belleudy et al., 2010) have been developed. These are non-contact devices collecting information indirectly and allowing continuous monitoring of bedload transport under a larger number of scenarios. However, these technologies are – to some extent – in the experimental phase, and require the collection of physical samples for calibration. Yet, these devices will most likely be those used in the future to collect information on bedload transport (Gray et al., 2010).

Bedload transport in sand-bed systems has been studied mostly in flumes, (Ashmore, 1988; Bagnold, 1966; Einstein, 1950; Engelund, 1966; Engelund and Hansen, 1967), but also with portable bedload samplers in large (Gaweesh and Van Rijn, 1994) and small rivers (Billi, 2011). And more recently by the use of surrogate techniques (Gaeuman and Jacobson, 2006b; Rennie and Villard, 2004). However, datasets on bedload transport in natural ephemeral sand bed channels are relatively rare and largely incomplete (Billi, 2011). This is given to the fact that sand bedded rivers are usually large rivers, with high water discharge and low slopes. In these settings, there are often large bedforms during higher flows, which make the continuous monitoring of bedload impractical (Holmes, 2010).

Among ephemeral rivers, bedload transport has been mostly studied in gravelly beds with higher bedload fluxes compared to their perennial counterparts (Larone and Reid, 1993); apparently, ephemeral steep sand bed rivers also have high bedload fluxes (Billi, 2011). As the channel bed in ephemerals is unarmoured (Lar-onne and Reid, 1993), hysteresis in bedload flux is rarely observed (Powell et al., 2003). Single thread ephemeral gravel bed rivers with moderate slopes exhibit a sequence of steeper bars and less steep, finer-grained 'flats' (Powell et al., 2012). In steep sand bed rivers, the bed tends to be flat, lacking bars, ripples and dunes; sheets are often observed in the channel bed (Billi, 2008).

This paper aims to provide continuous bedload observations on a fluvial system that has yet to be reported: a natural steep sand-bedded river with an ephemeral regime. We attempt to understand bedload flux and texture and their relations with hydraulic parameters. This objective is accomplished by acquisition and analysis of continuous bedload flux data obtained with two Reid-type slot

samplers installed in the stream bed. We aim to comprehend their spatio-temporal variation, as well as to which extent bedload flux varies with shear stress.

2. Study area

The Barranca de los Pinos is located in the Northern piedmont of the Guadarrama Mountains, Segovia Province in Central Spain. The underlying topography consists of a series of mesas and cuestras formed by Upper Cretaceous sediments and underlain by a crystalline basement of gneisses (Fig. 1). The plateaus are topped by a caprock of limestone and dolostone while the side slopes are clayey and gravelly sands that have been deeply dissected by gullies. The mesas and cuestras are covered by native forest (holm oak and junipers) and are grazed by sheep at certain periods of the year. The climate is Mediterranean with cool summers (Csb) according to Köppen classification (CNIG, 2004). It is characterized by a moderate average annual precipitation (680 mm) and temperature (11.4 °C).

The Barranca de los Pinos is typical of the gullied catchments of the studied area in terms of size, lithology and gradient of hill-slopes, and channel. It has been chosen to study different active geomorphic processes: gravitational processes in high gradient slopes, water erosion on low gradient slopes and sediment transport including bedload in the channel (Lucía et al., 2011). The catchment area (1.32 ha) is to a large extent gullied (90.4%), with high gradient slopes (29.9% of the gullied area has slopes steeper than 30°), narrow interfluvies and a high drainage density (0.041 m m⁻²). The longitudinal slope of the channel is 0.066 and its width at the monitoring site is 1.24 m, varying in the range 1–1.5 m. The gullied reach has friable, vertical sandy walls, but at the sampling site they are stable (Fig. 2); the slopes of the right and left banks are 29.4° and 78.8°, respectively and their height is approximately 70 cm. The channel bed lacks topography or undulations with a maximum 2 cm relief. It is of low sinuosity, 1.08, classified as straight to slightly sinuous (Leopold et al., 1964). The bed is formed by coarse, poorly sorted and positively skewed sand ($D_{50} = 0.555$ mm; $D_{84} = 0.995$ mm; $D_{90} = 1.42$ mm). Most (93.2%) of the bed material is sand sized, ranging from 0.062 to 2 mm. There are very small proportions of silts and clays (2.9%) and of gravel (3.9%), the latter being subrounded to angular quartzite lag deposits from the sandy facies or very angular carbonate rock fragments originally derived from the caprock and the associated colluvium.

Steep, sandy channels are uncommon in Nature, as finer grained rivers usually have lower gradients (Leopold et al., 1964). The studied channel is a rare combination of a sand bed and steep longitudinal slope. It exists here because the gullies are presently eroding fine-grained Upper Cretaceous sediments, deposited by large braided and meandering rivers in an estuary mainly by fluvial but also by tidal activity (Alonso, 1981), conditions which are indicative of low gradient channels. The gullied character of the

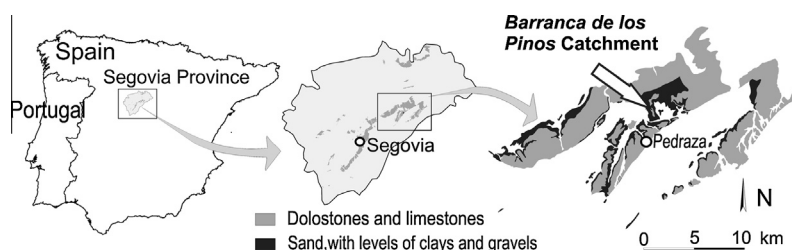


Fig. 1. Location of the study area. The mesas and cuestras are capped by limestone and dolostone (grey). The hillslopes, dissected by gullies, are underlain by horizontally-bedded silica sand deposits, with thin intercalations of clay and gravel (black).



Fig. 2. Upstream view showing the two Reid-type bedload samplers in the Barranca de los Pinos.

catchment provides an unlimited sediment supply to the channel. The study area has been described in detail elsewhere (Lucía et al., 2011).

3. Methods

3.1. Water stage

Water stage was measured at the study site by a vented pressure transducer located in one of the bedload slot samplers. Water density was assumed constant at 1043 kg m^{-3} .

3.2. Bed topography and texture

The topography of the channel bed was acquired from a point cloud data obtained with a Terrestrial Laser Scanner (TLS), which is based on Light Detection and Ranging (LiDAR) technology. The TLS is non-intrusive and has high precision; the instrument used (Leica Scan Station 2) measures up to 50,000 points per second with a 2 mm precision at a scanning distance $<120 \text{ m}$. Scanning was undertaken at least from two different locations to avoid shadowed areas (Buckley et al., 2008). The scanned channel reach is 12 m long (ten times the channel width) and it is located immediately upstream of the bedload sampler. The slope of the channel banks formed an asymmetric trapezoid, from which the hydraulic radius was calculated.

To determine the bulk Grain Size Distribution (GSD) of the bed-material, an 11.6 kg sample was scraped from the upper 12 cm of a 2 m^2 area of the channel bed. Only one area was sampled given the uniformity along the channel; nonetheless, this area is longer than the channel width. The sample was dried and sieved at 1/ intervals and lower-truncated at 0.062 mm (sand-silt split). Grain size descriptions were calculated using Gradistat (Blott and Pye, 2001).

3.3. Bedload

Bedload discharge was automatically and continuously monitored by two independent, cross-sectionally aligned Reid-type (formerly termed Birkbeck) bedload slot samplers (Reid et al., 1980). The cumulative mass of sediment entering each sampler is monitored by a vented pressure transducer connected to a pneumatic pillow filled with water, upon which an internal box is located. The hydrostatic pressure of the water column is monitored by a separate vented pressure transducer located between the outer and inner boxes of the right sampler. For a given time period, the pressure difference between the two sensors is due to the addition of mass of bedload entering the sampler (Laronne et al., 2003). Data from all the vented pressure transducers are read every 10 s and the average of three readings is logged every 30 s.

The volume of each inner box is 0.225 m^3 and was sized based on prior sediment yield assessment so that the box would not overflow during a typically frequent, low magnitude event (Lucía et al., 2011). Slot width is variable, the maximum (160 mm) representing 26% of the channel width. Ideally the slot width should be ten times larger than the size of the sediment to be sampled, and a compromise is required between the sampled sediment diameter, the representative width and the average sampling duration required for samplers to fill. During the sampling period the slot was set at 5 or 10 cm, much larger than the bed material grain size (50–100 times the D_{84}). The length of the slot was based on the saltation length for sand calculated as follows (Van Rijn, 1984):

$$\lambda_b/D = 3D^*0.6T^{0.9}$$

where λ_b is the saltation length with an accuracy of 50%, D is the particle diameter, D^* the dimensionless particle parameter defined as:

$$D^* = D_{50}[(\rho_s/\rho_w)g/v^2]^{1/3}$$

where m is the kinematic viscosity, q_s and q_w are the mass densities of sediment and water, g is gravity and T the transport stage parameter, which is defined as:

$$T = [(u^*)^2 - (u_{cr}^*)^2]/(u_{cr}^*)^2$$

where u^* is the bed shear velocity equal to $g^{0.5}/C^0$, C^0 is the Chézy coefficient related to the grains, and u_{cr}^* is the critical shear velocity according to Shields (equal to $[h_{cr} * ((q_s/q_w) - 1)g D_{50}]^{0.5}$). Applying this equation and using the D_{50} , 0.04 as the Manning parameter (Arcement and Schneider, 1989) and a maximum water depth of 30 cm, the saltation length was estimated to be 36 cm ($\pm 50\%$); therefore, the maximum length was predicted to be 54 cm. Indeed, the slot length at 65 cm is sufficient for the predicted transport conditions, thus having a 20% safety factor.

The sampler has a lateral window allowing observation of sediment stratification, hence enabling the collection of facies-based sediment samples. In all but few cases, sample weight was 100 times larger than the weight of the largest particle as recommended by Church et al. (1987). Bedload samples collected before April 2010 were dried and sieved with 1/ sieves and those collected after this date were sieved using 0.5/ sieves because it became evident that finer textural detail was required. The smallest sieve size used was 0.062 mm, essentially the lowest truncation. As these bedload samplers are of the recording type, the time during which a given layer of bedload sediment was deposited can be determined. This allowed correlating bedload texture with the channel-average shear stress, typifying the hydraulic conditions existing when the sediment was transported (Powell et al., 2001).

All vented pressure transducers (Druck PTX-1830) were pre-calibrated. The sensor measuring hydrostatic water pressure

has a sensitivity of 0.06% (according to the manufacturer). The sensitivity of this kind of weighting device comprising the pressure transducer and the pillow is estimated to be 0.3 kg given its size, (Laronne et al., 2003). However, sensitivity was also tested during calibration of this sampler. The calibration was undertaken with metal pieces of known weight larger than 9 kg, as well as smaller objects (0.25, 0.5, 1, 3 and 5 kg) while the sampler had a weight equivalent to (i) being filled only with water, (ii) when half-filled with sediment and (iii) when almost full with dry sediment. In all cases there was a significant linear correlation between the pressure registered and the weight introduced to the sampler. Regression lines were compared one to one with the regression line obtained with weights larger than 9 kg. The comparison was made using an ANOVA test, analyzing both the slope and the intercept. In this analysis, the slope is more relevant because it is the extent to which pressure changes with weight in the sampler. Obtained p-values show that there are no statistically significant differences among the slopes or the intercept at the 90% or higher confidence level to an accuracy of 0.25 kg. This value was used to analyse the data: increments of weight smaller than 0.25 kg were excluded in calculation of bedload flux.

The temporal stability of this type of pressure transducer has been shown to be quite good (Alexandrov et al., 2009). However, the properties of the pillow, which is made of neoprene, may not be similarly stable. Therefore, the weighting device was calibrated twice (in April of 2010 and February 2011), with results showing little change in the slope of the regression lines: 3.08% in the right sampler and 10.1% in the left sampler. Hence, for the events prior to August 2010 (the date in between the two calibrations) the regression line obtained during the first calibration was used to predict transported mass and that obtained with the second calibration was used thereafter.

3.4. Bedload data quality control

The reproducibility and quality of the bedload database is validated by the following procedure:

1. At the onset of some very small flow events calculated bedload flux rates were excluded due to two known errors: for a correct flux calculation the sampler has to be filled with water, which may take a few minutes (one to five) during small events. In other instances, the collected data were unrealistically high due to the effect of bed over-steepening that was produced by the process of cleaning of the upstream section of the sampler, after the previous event was recorded.
2. Slot sampling has been demonstrated in the lab (Poreh and Sagiv, 1970) and under field conditions (Habersack et al., 2001) to be 100% efficient while sampling sand to gravel bed-load as long as they are not nearly full. When the volume of sediment in the sampler approaches about 80% of its capacity, the efficiency decreases due to internal vortices that can remove some of the sediment from the samplers (Habersack et al., 2001). Data collected under these conditions were removed due to sampling inefficiency.
3. During the latter stages of some hydrograph recessions, water depth over the sampler decreased much slower than expected, most likely due to sand deposition over the sampler or mud deposition within the sampler on the pressure transducer. This effect was corrected by adjusting hydrograph recession up to the inflection point to an exponential equation. From the inflection point onwards, bedload data were correlated with depth recalculated by the exponential equation.

4. Results

4.1. Hydraulics

The Barranca de los Pinos is a truly ephemeral channel. Water was present in the channel during 1.98% of the monitored time, merely 11 of 556 days. Twenty-four flow events were registered during 18 months, June 2009 – January 2011 (Table 1). All the events were generated by rainfall with a return period smaller than two years. Three events (9, 22 and 23) did not register accurately as they were small and short, with difficulties that occur at the beginning of some events (see Section 3.5) affecting the entire event dataset; these were excluded.

Maximum registered water depth was 15.5 cm (averaged every 30 s). Median water depth was 2.6 cm, and the first and third quartiles were 1.0 cm and 4.5 cm respectively. The longitudinal slope of the channel is considerable (0.066), so despite the shallow water depth, shear stress was quite high, with a maximum instantaneous (30 s) value of 10.7 N m^{-2} . Channel average shear stress was calculated as (Du Boys, 1879):

$$\tau = \rho_w d S g$$

where S is shear stress (N m^{-2}), d is water depth (m) and S is bed slope (nondimensional).

4.2. Bedload flux

During most of the events bedload transport was initiated soon after water appeared in the channel. On average the onset occurred within 4.6 and 6.2 min in the right and left-hand samplers, excluding few events in which the hydrograph rise was exceptionally slow (inclusion of these events increases the respective average gaps to 13.1 and 26.6 min).

One of the limitations of the Reid bedload sampler is its finite volume. However, given the small size of the catchment and the brevity of some of the bedload-generating flow events, there were nine events when both samplers did not fill entirely, and one additional event during which only one of the samplers did not entirely fill. Bedload flux was monitored at peak flow in six of 12 events when the samplers had filled.

When samplers were full the maximum cumulative mass varied between the samplers (Table 1). This value is the integration of bedload fluxes for the sampling period before sampler efficiency decreases. As bedload fluxes lower than the sensitivity (0.25 kg in a given time interval) are excluded, the samplers may contain more sediment than that calculated as the total cumulative mass.

Measured bedload fluxes were high for both samplers; the highest 30 s recorded values were 25.4 and $19.5 \text{ kg s}^{-1} \text{ m}^{-1}$ in the left and right sampler, respectively. During the monitoring period, 2375 values of 1-min averaged bedload flux were obtained; their median, first quartile and third quartile were 0.33, 0.16 and $0.70 \text{ kg s}^{-1} \text{ m}^{-1}$. In a general sense, the relation between bedload flux and water depth may be simple or complex (Cohen et al., 2010). In the analysed database (1-min averaged), the relation between the entire bedload flux vs shear stress is very scattered (Fig. 3a). However, lower scatter characterizes some events (Fig. 3b).

4.2.1. Temporal variation

Given the large scatter in bedload flux, the variability of bedload transport rates is examined by evaluating two types of temporal variability: hysteresis (variations in bedload flux on rising vs falling hydrograph limbs) and waves (periodic fluctuations in bedload flux unrelated to changes in flow stage).

Table 1
Summary of the monitored bedload-generating flow events (June 2009 - January 2010) in the Barranca de los Pinos.

Event	Sampling date	Max. water depth	Max. water depth before the sampler filled	Max. shear stress	Max. cumulative mass (LS)	Max. cumulative mass (RS)	Max. bedload flux (LS)	Max. bedload flux (RS)	Time gap: beginning of flow and bedload (LS)	Time gap: beginning of flow and bedload (RS)
		mm	mm	N m^{-2}	kg	kg	$\text{kg s}^{-1} \text{m}^{-1}$	$\text{kg s}^{-1} \text{m}^{-1}$	min	min
1	01/10/2009	7	7	4.9	9.3	3.7	0.2	0.1	20.5	23
2	22/10/2009	13	13	9.1	22.0	5.1	0.8	0.1	2.5	3.5
3	02/12/2009	68	68	47.7	120.8	156.6	1.1	1.5	1.5	1.5
4	23/12/2009	134	134	93.6	88.8	118.4	13.8	1.5	11.7	7.5
5	15/01/2010	110	110	76.8	178.1	151.4	5.6	3.5	5	1.5
6	19/01/2010	50	48	35.6	173.3	—	2.1	—	42.5	—
7	05/02/2010	23	23	16.0	0	134.1	0	1.2	—	176
8	19/02/2010	69	69	48.9	180.3	169.2	3	1.5	10	4
10	16/03/2010	77	77	54.1	85.8	145.8	1.7	1.5	366	31.5
11	16/04/2010	40	40	28.1	80.9	23.44	5.3	1.49	0.5	2
12	11/05/2010	60	60	42.6	183.6	194.8	10.4	5.9	1	1.5
13	14/05/2010	54	54	38.2	120.5	172.9	5.6	19.45	12	0.5
14	01/06/2010	47	47	33.2	37.5	168.9	2.5	3.6	5	0.5
15	15/06/2010	155	77	107.0	167.4	124.3	7.6	8.4	3	0.5
16	06/07/2010	57	57	40.4	56.6	137.1	5.8	4.2	1	1
17	06/09/2010	80	80	56.2	168	163	19.9	6.7	11.5	0.5
18	24/09/2010	155	155	107	199.8	199.9	25.4	19.3	0.5	0.5
19	11/10/2010	36	36	25.2	91.9	132.4	2.7	3.1	0.5	0.5
20	01/11/2010	50	50	35.4	166	172.5	4.4	2	19	4
21	12/11/2010	63	63	44.7	178.7	185.5	8.4	3.5	0.5	0
23	08/12/2010	61	61	43.3	192.2	186.1	3.6	2.8	77	2.5

The sampler was filled since the previous event, therefore bedload was not monitored LS left sampler; RS – right sampler.

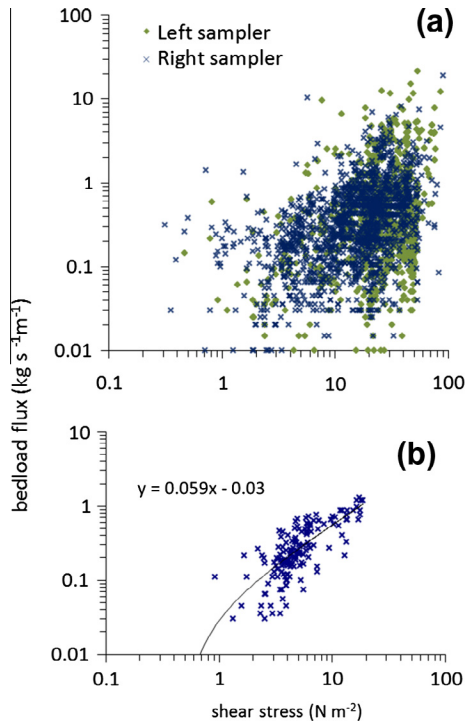


Fig. 3. Scatter graph of bedload flux vs shear stress for all bedload flux data in both samplers (a); example of event (08/12/2010, event 23, right sampler) when bedload flux is coherent with shear stress; $r^2 = 0.74$ (b).

The rate of change of water stage is considerably more rapid during the rising limb than during the recession in many of the events. Hence most of the bedload flux data were obtained from recessions by virtue of this portion of the hydrograph lasting long-er (Fig. 4). Observed instances of hysteresis in the variation of bed-load flux with water depth are without exception clockwise, with higher rates of transport occurring during rising stage than during flow recession. This was documented in eight and nine events among twenty in the left and right sampler, respectively. Bedload hysteresis was observed mostly in summer and autumn. The proportion of events with hysteresis is highest (83%) in the summer, and lowest (20%) in spring, followed by winter (30%) and some-what more (42%) in autumn (Fig. 5).

In some of the monitored flow events, or parts thereof, bedload flux corresponded well to water depth (Fig. 6a). At other times, large oscillations of bedload flux (waves) occur both, during steady flow (Fig. 6b) and unsteady flow (Fig. 6c). Oscillations were documented in eight and nine events in the left and right samplers

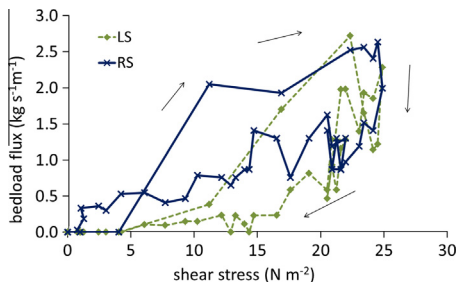


Fig. 4. Example of clockwise hysteresis (direction of arrows) during event 19 (11/10/2010). LS = left sampler; RS = right sampler.

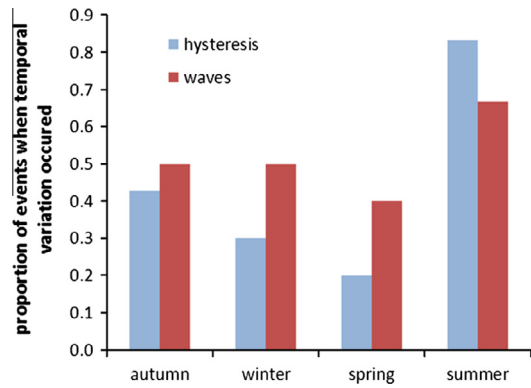


Fig. 5. Seasonality of the two kinds of temporal variation of bedload flux. Wave occurrence varied seasonally less than did hysteresis, the latter was more frequent in summer.

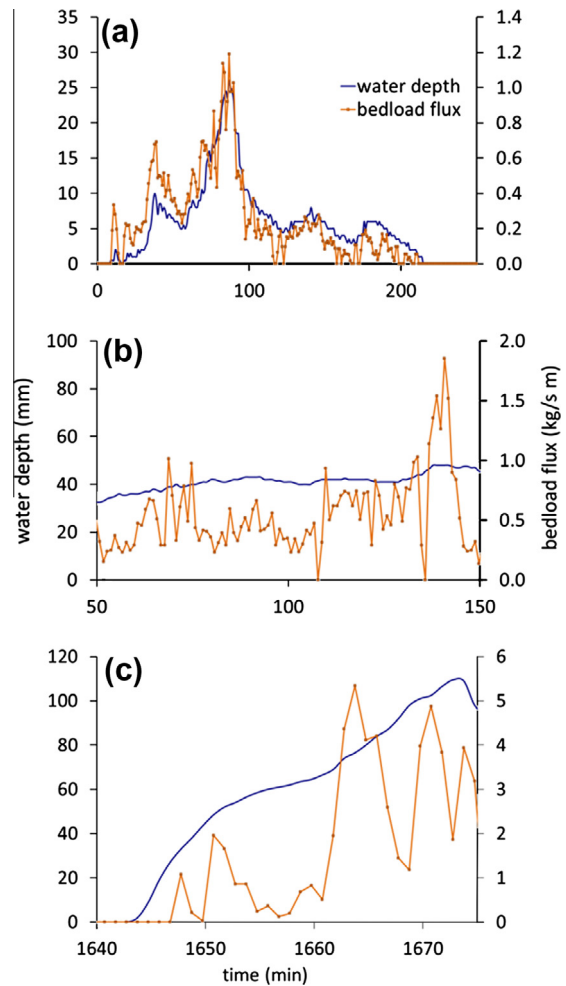


Fig. 6. Flow event 23 on 08/12/2010, when bedload flux in right sampler varied with water depth – see Fig. 3b. (a) Flow event 6 on 19/01/2010 when bedload flux in left sampler varied temporally while water depth remained essentially stable (b), flow event 5 on 15/01/2010 when bedload flux in left sampler varied temporally in a wave-like manner during quasi-constant increase in water depth (c).

respectively, indicating the frequency of waves in bedload response; the presence of waves is independent of water depth. Notably, hysteresis and waves do not necessarily occur simultaneously. Wave occurrence varied seasonally less than did hysteresis. Waves occurred in 40% of the spring events and in 67% of the summer events (Fig. 5).

4.2.2. Spatial variation

Spatial variation of bedload flux was described based on the evaluation of registered bedload flux differences between samplers and, separately, their temporal responses. Considerable spatial variation (differences in bedload rates of more than the 50% or more than 5 min of interval in bedload flux registration) occurred in 11 of 20 events. In nine of the 11 events, bedload flux occurred later in the left sampler compared to the right sampler. Bedload entrainment was recorded in the left sampler when water depth attained a minimal threshold depth in the range 17–35 mm. The largest spatial differences in bedload flux occurred in shallow, bedload-transporting flows during hydro-graph rise (Fig. 7).

4.3. Bedload texture

Bedload collected in the Reid-type samplers showed an alternation of coarser and finer-grained sedimentary layers. Bedload texture was analysed from 276 facies-based bedload samples. Correlating the thickness of the various facies with their cumulative weight allowed inferring when the sample was collected (Laronne et al., 2003). The GSD of the samples were averaged and compared to the corresponding shear stress in 5 N m^{-2} bins. Interestingly, the GSD of bedload is unrelated to shear stress (Fig. 8) indicating that selective transport cannot be deduced from these data. The range in D_{50} variation is smaller than that for D_{90} , but the relative variability is similar (Fig. 8),

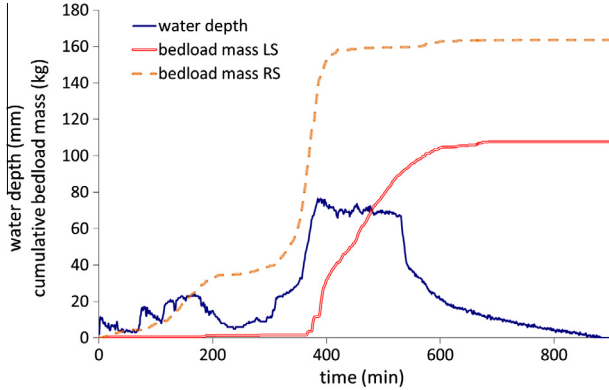


Fig. 7. Example of bedload-generating flow event 10 (16/03/2010) when considerable spatial variation in bedload flux occurs. Water is initially very shallow, supplying bedload only to the right sampler. Overcoming a threshold in water depth, bedload is thereafter also transported on the left side of the channel.

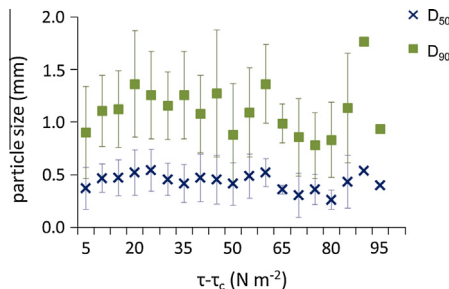


Fig. 8. D_{50} and D_{90} vs $S - S_c$ (shear stress minus the critical shear stress in both samplers and averaged for 5 N m^{-2} bins. The critical shear stress was calculated using the Meyer-Peter and Müller (1948) non-dimensional critical shear stress (0.047).

as expected given their respective sizes (Whitaker and Potts, 2007).

4.4. Morphotexture of the channel bed

The explanation of (1) the alternation of GSD facies within the sampler despite non-selective bedload transport, as well as (2) the spatiotemporal variation of bedload flux while flow depth re-mained essentially constant, appears to depend on the character of channel bed morphology. Comparison of the median water depth with the relief of what at first appeared to be a simple flat channel with minute topographic differences, in fact shows that both are of similar magnitude. A zoom into the ephemeral channel bed after the occurrence of a bedload-generating flow event re-reveals that the bed is comprised of bedforms with an apparent braided pattern (Fig. 9a). To describe the characteristics of the channel bed in detail, a topographic survey was carried out with the Terrestrial Laser Scanner (TLS). A 10 m channel reach of a tributary gully of the Barranca de los Pinos was selected for this survey because the topographic characteristics are essentially identical in both channels, and because the Barranca bed was disturbed by ani-mal trampling which destroyed its micro-topography. The scanned tributary joins with the main stem immediately downstream of the Barranca monitoring station.

The DEM obtained with the high resolution (1 mm) topographic survey demonstrates that the channel has a well-defined braided pattern (Fig. 9c) with complex bars on which chutes are developed, having an average length, width and height of 91, 21 and 1.2 cm respectively. The average braiding index, defined as the number of anabranches (arrows in Fig. 9d) per cross section (Egozi and Ashmore, 2008), is 3.5 (Fig. 9d).

Considering the presence of these bedforms, a new sampling strategy was undertaken to better characterize channel texture (Fig. 9b). Bar and anabranch surfaces and subsurface were separately sampled, as was the general subsurface (Fig. 10a). The sampling of the surface was undertaken by carefully scraping one-grain layer of surface sediment. The subsurface was characterized by a bulk sample representing 1–2 cm of the subsurface sediment. A large (3.4-fold) difference in grain size occurs between the D_{50} of the surface of anabranches (0.39 mm) and that of the bars (1.30 mm). That bar surfaces are coarser-grained than the subsurface indicates that the bar surface is affected by a phenomenon of segregation which is absent in the anabranches. The median of the bar subsurface tail is 20% finer than the respective bar head, revealing the existence of a bar-scale sorting process.

Comparing the GSD of the different parts of the channel with the samples of the bedload retained in the samplers shows that bedload texture for many of the samples was both coarser than that of the anabranch subsurface and finer than that of the bar surface (Fig. 10b). Nearly half (44.5%) of all bedload samples were finer-grained and the rest, a slightly larger fraction, coarser grained than the anabranches. Only two bedload samples had a larger D_{90} than the respective centile of the bar surface. The frequency of movement of the different sizes of bedload was analysed considering the individual sampling duration and the total event sampling duration of each of the right (RS) and left (LS) samplers (Fig. 10b). The GSD of the bedload collected in both samplers is almost identical to the GSD of the average of the channel to 2 cm depth, demonstrating that equal mobility characterized the entire duration of bedload monitoring. However, since the analyzed bedload samples show an alternation of coarser and finer-grained layers, and bedload transport was not selective with reference to increasing shear stress (Fig. 8), it is suggested that the observed variations in GSD of the bedload are related to bed-form movement.

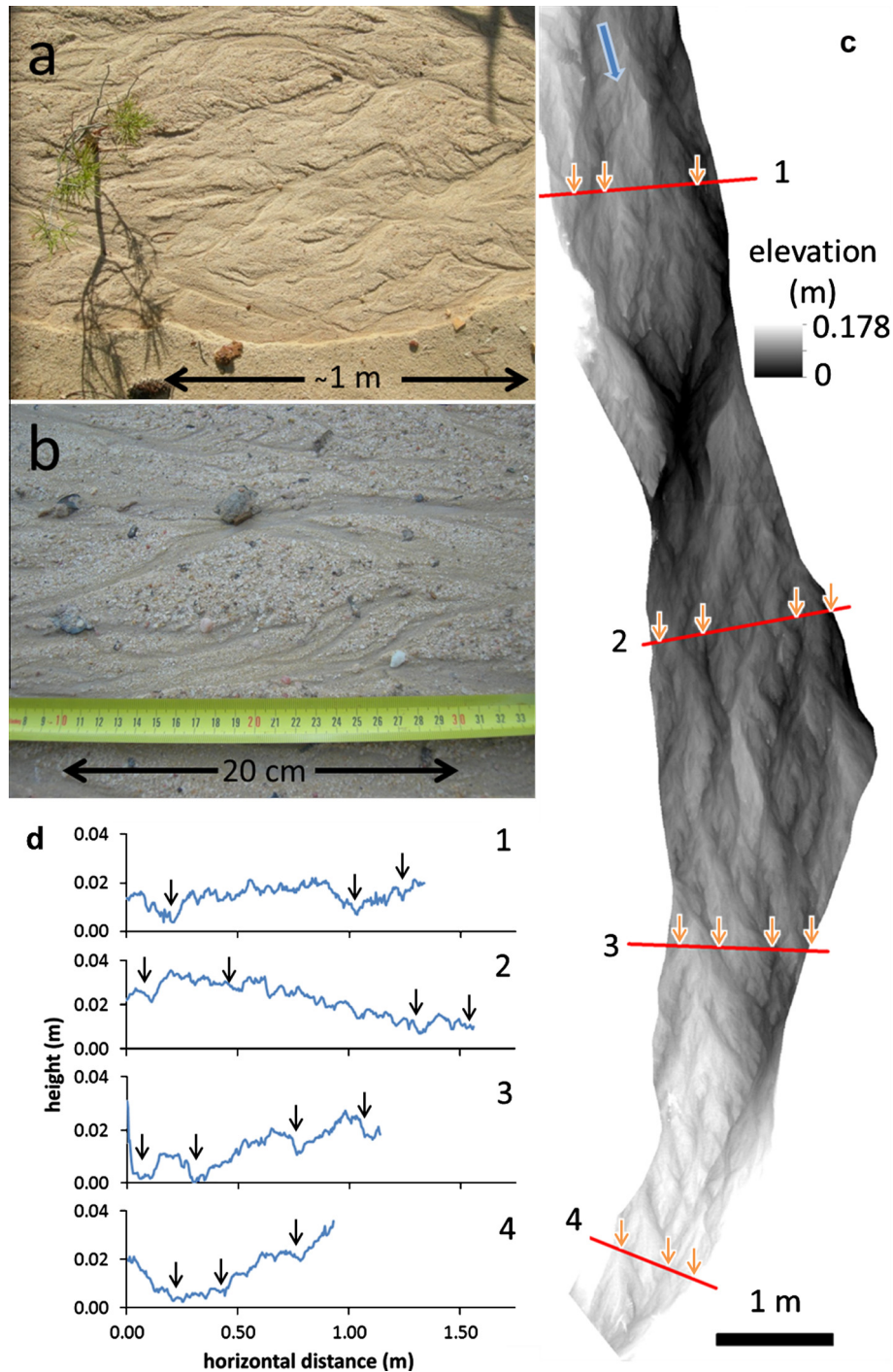


Fig. 9. Detail of the miniature braided pattern of the Barranca channel soon after a bedload-generating flow event occurred (a), detail of the coarser bars and finer-grained anabranches (b), high resolution DEM (0.4×0.4 mm) of a channel reach after detrending the longitudinal slope (c), showing the braided pattern, the individual bedforms (complex bars with chutes developing on top of them anabranches surrounding them), and the location of cross sectional profiles along the braidplain dominated by bars and anabranches (marked with arrows) (d).

5. Analysis

5.1. Prediction of bedload flux

In an attempt to determine the applicability of bedload equations to small, steep sand bed channels, monitored bedload flux data were compared to selected bedload equations (Fig. 11). Ten minute averaged data were used to diminish temporal variability

inherent in bedload transport (Ergenzinger et al., 1994). The ratio between calculated and observed values ranged as much as three orders of magnitude.

The Smart and Jaeggi (1983) equation, established for flows on steep slopes and nearly uniform sediments including sand, was first compared with our data. The formula considerably overestimates with a median calculated/measured ratio equal to 16 (Fig. 11). The Smart and Jaeggi formula was established for straight

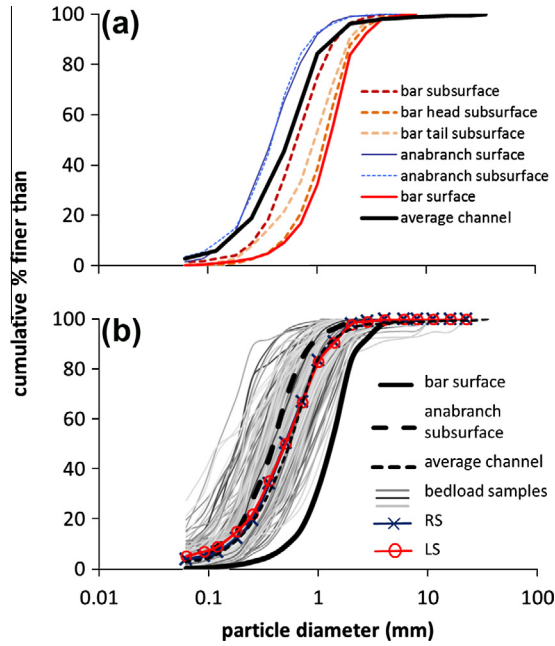


Fig. 10. Texture of various riverbed units, with differences of one order of magnitude in the texture of anabranch and bar surfaces (a). Grain size distributions of bedload samples (thin light grey); the bold dashed black line represents the average anabranch subsurface and the bold black line the bar surface. Bedload texture is on average well represented by the average anabranch subsurface. Individual bedload samples are considerably finer-grained than the subsurface and few others considerably coarser, approaching that of the surface of bars. Time-weighted mean GSD of bedload (RS = right sampler; LS = left sampler), is almost identical to the average channel GSD (b).

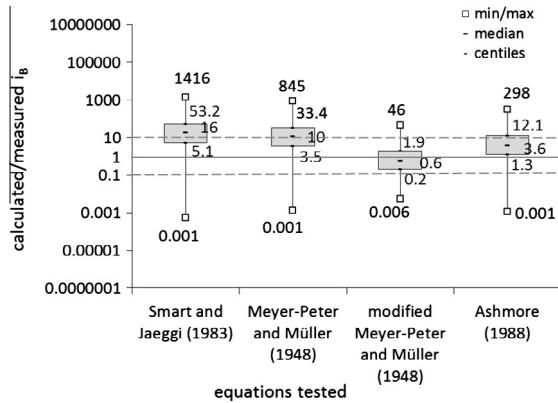


Fig. 11. Ratio of calculated/measured 10-min averaged bedload flux (I_b) in both samplers. Bars indicate ranges; boxes indicate the 25 and 75 centiles; the median is represented by a dash in the boxes.

channels with minimal bedforms, whereas in our study bedload was measured in braided channels, where form resistance is far from negligible.

Despite being developed for lower slopes and coarser sediment, the well-known Meyer-Peter and Müller or MPM (1948) formula was also examined as it has become a standard for estimating bed-load under a variety of settings. Bedload was overestimated with a median ratio of 10 (Fig. 11). An improved fit, the range of discrepancy decreased to about two orders of magnitude (corresponding to a median ratio of one) was obtained by including the roughness correction $n^0/n = 0.4$ (where n^0 is the grain roughness and n is the total roughness); however flow velocity data were unavailable to assess the appropriateness of this value.

The Ashmore (1988) equation was developed from data obtained in flume experiments with conditions similar to the ones present in the Barranca de los Pinos channel (sand and small gravel $D_{90} = 4$ mm, though with a gentler slope 0.01–0.015). It was developed as a model for braided gravel bed rivers. The results show an overestimation, with a median calculated/measured ratio of 3.6 (Fig. 11). This is not as large as other ratios, well within the -0.1 to 10 range recently used for similar comparison of bedload equations (Recking, 2010) in consideration of the uncertainties of the empirical equations and of the queries associated with bedload measurements (see hereafter). This equation implicitly takes into account form resistance associated with the braided pattern, with no requirement for an a priori hydraulic correction as with MPM. However, it was derived for the mean bed shear stress (calculated from the cross-sectionally averaged depth and width), whereas in this study, local depth (that over the right slot sampler) was used.

In summary, such equations were expected at best to predict the median bedload flux, though with admittedly large confidence intervals. Certainly none of these and other tested bedload formulae can be expected to reproduce the large variations about median (or mean) bedload fluxes, fluctuations which are inherent to bed-load transport in multithread channels.

5.2. Fluctuations in bedload flux

One of several reasons for variability in bedload transport is the fluctuating nature of boundary conditions at a given location: slope (S), grain diameter (D) and flow depth (approximately equal to the hydraulic radius (R) for shallow flows); these are the building blocks of the Shields parameter or non-dimensional shear stress (τ^*):

$$\tau^* = R S / [D((\rho_w/\rho_s) - 1)]$$

where R is hydraulic radius. These parameters varied in time and space in this study as follows:

- 150% For sediment diameter when considering maximum and minimum D_{50} measured in the different parts of the channel (Fig. 10a).
- $\pm 0.8\%$ Of the average slope the maximum fluctuation observed in some flume experiments with high longitudinal slope (9%) (Recking et al., 2009).
- Water depth minus a range from 0 to 3 cm; 3 cm is the maximum bar height in the cross section (Fig. 9d).

It is relevant to note that the calculated variations in these parameters do not completely explain the large variability of observed bedload flux. Indeed, bedload fluctuations are also linked to variation in the supply of sediment and occur in rivers under steady flow (Ashmore, 1988; Cudden and Hoey, 2003; Ergenzinger et al., 1992; Gomez, 1983; Gomez et al., 1989; Recking et al., 2009; Turowski, 2010).

To determine whether such fluctuations occur and also their nature, frequencies of the temporal variation of bedload flux and water depth were analysed using a Fourier transformation (Recking et al., 2009). For this analysis, only data from the right bedload sampler were used, because the vented pressure trans-mitter recording water depth is located in the right slot sampler, and there are considerable variations in water depth across the channel at shallow flows. Most of the events had a short duration, which prevented undertaking a thorough Fourier analysis for all the events. Four events (7, 8, 20 and 23 Fig. 12) had a duration longer than 100 min, considered to be sufficiently long to permit a time series analysis. These were sampled at 1 min interval. The four events represent a range of flow characteristics while bedload flux remained within a similar range of values. Although a clear peak of frequencies is not observed, all the bedload flux

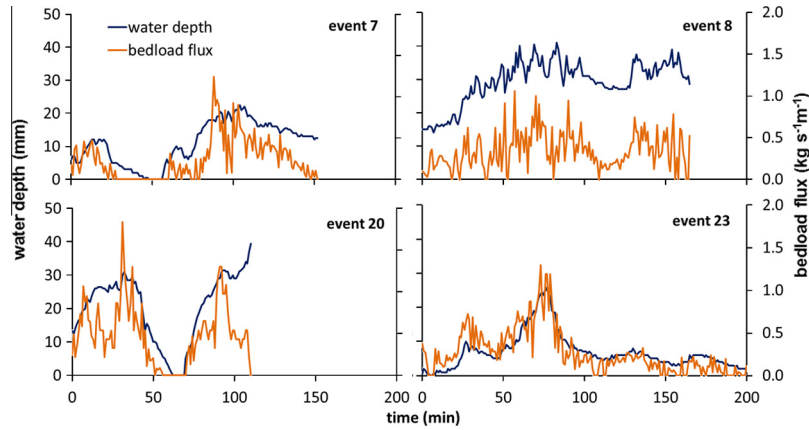


Fig. 12. Temporal variation of bedload flux (right-sampler) and water depth during events when monitoring duration exceeded 100 min.

signals have an identical spectral signature (Fig. 13b) despite the different frequency spectrum of flow depth (Fig 13a). This suggests that fluctuations are in part controlled by internal mechanisms such as bedform movement. While there were no clear peaks in the bedload signal there was a progressive evolution covering all frequencies, indicating that the phenomenon responsible for fluctuations is not discrete, but continuous; e.g., bedload sheet movement or the braiding pattern, which incessantly changes over time.

6. Discussion

The obtained data allows characterizing bedload flux and GSD and its relation with the shear stress in this environment, revealing a complex system with several particularities.

6.1. Bedload flux and hydraulics

The Barranca de los Pinos is distinctly ephemeral, with water and sediment movement occurring during only about 2% of the study period, similar to many other ephemeral streams (Reid et al., 1998). During this period, the mean water depth in the channel was 16 mm, ranging from 1 to 155 mm. Despite the shallow flow, bedload fluxes were high; the 1st and 3rd quartiles were 0.33 and 0.70 $\text{kg s}^{-1} \text{m}^{-1}$ but maxima of more than 20 $\text{kg s}^{-1} \text{m}^{-1}$ were registered. These bedload fluxes are higher than fluxes

continuously monitored in perennial gravel bed rivers in different environments, ranging between 0.001 and 1 $\text{kg s}^{-1} \text{m}^{-1}$ with maxima rarely higher than 1 $\text{kg s}^{-1} \text{m}^{-1}$ (García et al., 2000; Habersack et al., 2001; Laronne and Reid, 1993; Mao et al., 2010; Milhous, 1973; Rickenmann and McArde, 2007; Vericat and Batalla, 2010). They are also higher than the few measured rates in small flow events in an ephemeral sandy river having a steep longitudinal slope, the Gereb Oda (Billi, 2011) where measured bedload ranged from 0.01 to 1 $\text{kg s}^{-1} \text{m}^{-1}$.

Bedload fluxes obtained in the present study are comparable to those measured in sandy gravel bed rivers draining active volcanic terrain such as Mt. Pinatubo after its eruption (Hayes et al., 2002) with rates from 0.1 to 2.2 $\text{kg s}^{-1} \text{m}^{-1}$ and to upland ephemeral, gravel bed rivers in the Israeli desert: Nahal Eshtemoa (Reid et al., 1998); Nahal Yatir (Reid et al., 1996) and Nahal Rahaf and Qanna'im (Cohen and Laronne, 2005), where respective transport rates of 0.1 to 2.2, 0.01 to 8, 0.1 to 37 and 0.1 to 15 $\text{kg s}^{-1} \text{m}^{-1}$ have been measured, in four ephemeral gravel bed rivers with an identical method and a 1-min averaging duration of bedload flux. In fact, bedload fluxes in the Barranca were in a similar range and produced by the same magnitude of shear stresses as in these ephemerals. While channel types are distinct there are similarities: they have a segregated coarser bar surface, almost twice the median size of the subsurface (1.71 and 1.98 times coarser in the Nahal Yatir and in the Barranca respectively). However, in the Barranca de los Pinos the slope is steeper whereas sedimentary grain size and water depth are at least one order of magnitude smaller. The reasoning for the high Barranca bed-load fluxes is thought to be the ephemeral character of the channel (Laronne and Reid, 1993), the fine texture of the channel bed, the steep longitudinal slope and the high sediment supply (in the sense of Dietrich et al., 1989).

Ephemeral rivers continuously monitored using Reid bedload samplers have been shown to have a high correlation between channel average bedload flux and cross-sectional averaged shear stress. Where cross-sectional variations do occur, they are ascribed to variation in local shear stress (Powell et al., 1999). The dependence of total bedload yield on average shear stress is also strong in miniature braided sandy channels formed in flumes (Ashmore, 1988). However, in most of these relations a substantial scatter was evident, as is in the channel of the Barranca de los Pinos. In this site, the scatter is explained as a consequence of two types of temporal variation (hysteresis and sediment waves) and spatial variability.

Despite substantial spatial and temporal scatter, measured bedload flux data were compared to a set of standard bedload equations to evaluate the ability of these to predict rates of bedload flux for braided sandy streams. Standard bedload equations tend

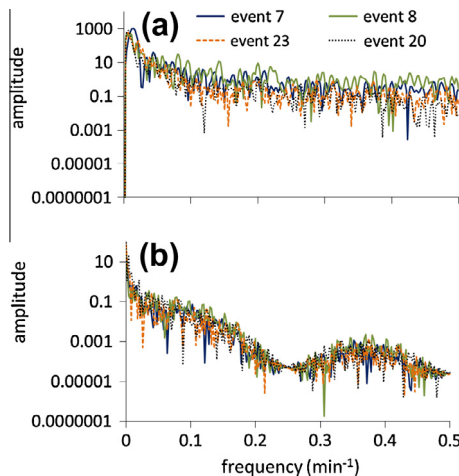


Fig. 13. Evaluating the presence of a dominant frequency of bedload flux waves based on Fourier analysis of bedload data for events when monitoring duration exceeded 100 min; water depth signal (a) and bedload flux signal (b).

to underestimate bedload sediment yield when they are used with width-averaged input data because they are non-linear (Gomez and Church, 1989; Ferguson, 2003; Paola, 1996); this is particularly true for braided rivers with highly irregular sections (Bertoldi et al., 2009; Nicholas, 2000). The contrary (overestimation) was observed here when estimates from the Meyer-Peter and Müller and Smart and Jaeggi equations were compared against the Barranca de los Pinos database. This can be explained by two reasons: first, calculations were not made with the width-averaged data, but with a local shear stress computed from the depth measured at the right slot sampler. Second, the computed shear stress was not corrected for form-induced resistance, which was likely higher than the grain shear stress. The empirical Ashmore (1988) equation developed in a flume for gravel-bedded braided rivers predicts better the bed-load flux response, even though it is to be applied to channel average values rather than to local bedload flux.

6.2. Morphotexture of the channel

The Barranca bed topography, as well as the temporal and spatial variability in bedload flux and its texture, point to the existence and importance of bedforms. Bedforms are a result of the interactions between coarse and fine fractions during bedload transport of poorly sorted bed material (Dietrich et al., 1989), as observed in experiments at constant water discharge in flumes (Ashmore, 1988; Iseya and Ikeda, 1987; Nelson et al., 2009; Recking et al., 2009) and in sandy natural rivers (Whiting et al., 1988).

The observed bedforms in the channel of the Barranca de los Pinos could be bars or sand sheets. Given their average dimensions: 91 cm long and 1.2 cm thick, they are to be considered bars since their size is larger than the dimensions given for bedload sheets a length of 100–600 grains and one or two grains thick (Whiting et al., 1988), which, scaled to the studied channel, would be equivalent to 0.6 m long bedforms with a thickness of 2 mm. The bedforms are also more extensive than bedload sheets observed in the Gereb Oda, (Billi, 2011). The thickness of the bars in the Barranca is almost half of the median water depth, similar to the height of bedforms described as bars that were present in flume runs of braiding using sand (Ashmore, 1982). We have observed the activity of these features during bedload generating events: they move and reform similar to bars observed in flumes, but we have insufficient observations to state more.

From the available information, we deduce that the Barranca has two bedforms: bars (based on the topography and bed material texture) as well as somewhat smaller bedload sheets (based on oscillations/waves of bedload flux with time and the texture of the bedload) moving over more stable bars in a braided pattern. This pattern has been observed in flume experiments (Ashmore, 1988; Hoey and Sutherland, 1991) and in gravel bed rivers (Church and Jones, 1982; Rice et al., 2009). Indeed, bars are formed by the accumulation of successive bedload sheets (Rice et al., 2009). The topographic signature of the sheets is not distinguished in the field nor in the TLS-based DEM; nonetheless, they do contribute to the roughness detected on the bars (Fig. 9c). It is apparent that bars are reshaped by the flow in the anabranches during the recessions as we have observed in the few instances while present during recession and as suggested elsewhere (Billi, 2008).

The bar surfaces, which are coarser-grained relative to the subsurface, indicate the occurrence of segregation, a phenomenon observed in some gravel-bed channels and explained by en masse deposition, particularly of the coarser sedimentary particles (Duncan and Laronne, 1998) or else by the winnowing of fines (Leopold, 1994). The equal mobility and the non-size selective transport (Batalla and Martín-Vide, 2001) of Barranca sandy bedload indicates that the segregated surface is unstable (in the

sense of Gomez, 1984). Indeed the one-particle diameter surface layer of the bars is not well packed, having no observed interlock. The coarser surface has been described as resulting from bedload sheet transport (Recking et al., 2009). The latter is assumed to result from a kinetic sieving process, being a very efficient sorting mechanism which occurs in a moving layer, where the fine fraction is driven downward into the sediment deposit and thereby produces a coarse bed surface (Frey and Church, 2012).

Compared to the segregated, sandy Barranca bars, those in ephemeral gravel bed rivers have been shown to be to a large extent unsegregated (Laronne et al., 1994). The miniature anabranches which are unsegregated, typical of other ephemeral systems (Hassan et al., 2006; Laronne et al., 1994), have been explained to form by high sediment yields and rapid recessions that minimize sediment winnowing. The processes occurring on the channel bed during bedload transport appear to be similar to those described in ephemeral gravel bed rivers. That the subsurface in the bar tail is finer-grained than in the bar head reveals that bar-scale sorting processes also occur, however apparently not as efficiently as in gravel-bed rivers (Rice and Church, 2010). The lesser textural gradient may owe its character to the finer overall texture and the better sorting in the Barranca de los Pinos.

6.3. Interaction between morphotexture and bedload flux variability

Explanations for clockwise hysteresis in bedload transport are manifold: long lasting or very intense flow exhausting the stored sediment, limited available sediment supply (Humphries et al., 2012; Williams, 1989), sediment delivery from the channel bed and banks or areas adjacent to the channel rather than from up-stream sources and lack of channel bed armouring (Hassan et al., 2005). However the Barranca has virtually unlimited sediment supply, so limitations on sediment availability cannot explain the hysteretic response. One process that may generate the clockwise hysteresis is the destruction of the low relief of the Barranca bars between flow events. If so, bed roughness will be lower and water velocity higher at the onset of the following event, which may explain the clockwise hysteretic behavior of bedload flux. As bedload transport commences, bedforms are reformed to the braided pattern, increasing roughness and decreasing bedload rates.

There are several mechanisms through which bedforms may be disturbed between events. Observed animal trampling between flow events did destroy bedforms above the site. Trampling increases roughness by giving rise to hoof-generated indentations. Increased roughness due to trampling would thus result in lower bedload fluxes during the rising limb, so trampling cannot explain the observed results. A second relevant mechanism is the loss of the minuscule cohesion of the sandy surface during a dry spell between flow events, when the subdued bedforms are blurred by small gravitational movements along their borders, or by aeolian activity, in part removing sediment from the bars and filling the minute anabranches (Good and Bryant, 1985). This could also explain why the braided pattern of the channel was unnoticed before initiating the monitoring of water and sediment in the Barranca. Our data stands to support the second above mentioned mechanism, because hysteresis is only present in events occurring at least eight days after a preceding event. This may explain why the proportion of hysteretic events is higher in summer than in other periods of the year, since in this season rain events are more sporadic and the channel is dryer, meaning less cohesion in the sandy bed surface. Relevantly, at the onset of some events, the GSD was similar in both samplers, which may point to the existence of as yet undeveloped bedforms.

The clockwise hysteresis in the Barranca cannot occur only due to a reduction of the roughness during dry periods since this has been documented in natural rivers (Gaeuman, 2010) and also un-

der controlled flume conditions, with unlimited sediment supply and nonuniform sediment. In the latter, the explanation has been the reorganization of the bed surface, reducing the mobility of the finer sediments, thereby decreasing bedload flux during the falling limb of the hydrographs (Mao, 2012). Therefore, reorganization of the bed surface at the studied site may also reduce the mobility of the finer sand, since the bar surfaces are coarser.

The observed spatial variability in bedload flux, when bedload was registered in the left sampler only when water depth passed a threshold (see example Fig. 7), may occur due to the presence of a bar, the bifurcation of which blocks water from flowing to the left side at shallow depths. When water depth exceeded bar height, bedload was registered over both samplers – over the entire 'braidplain' – reducing lateral differences in bedload flux. This phenomenon is not always observed, possibly because the bar was not developed in that position or because it was blurred by inter-event drying or trampling, as explained above.

7. Conclusions

Local but continuous bedload flux data obtained in the Barranca de los Pinos are the first available for natural sand-bedded channels. Their availability allow a glimpse into the understanding of bedload transport in steep sandy channels, making headway in the identification of the sources and causes of temporal and spatial variability.

1. Recorded bedload fluxes are among the highest measured to date comparable to those registered in upland ephemeral gravel bed rivers or rivers draining active volcanic landscapes, produced by high longitudinal slopes with fine-grained channel bed material, indicating high supply of sediment.
2. The local bedload flux vs local shear stress database is characterized by a very large scatter. Comparisons with bedload equations, even if developed for similar, though channel average conditions, will predict a relationship that can differ as much as an order of magnitude from measured values.
3. The scatter in bedload flux is produced by the existence of often unrecognized miniature bedforms: bedload sheets moving over a subdued braided pattern, thereby producing temporal and spatial variability in bedload flux.
4. These bedforms move and evolve during bedload-generating flow events, leading to sediment waves interpreted as miniature bars with overriding bedload sheets. The presence and emergence of very small central bars is the mechanism by which spatial variability in bedload flux develops, similar to such processes in large braided rivers. The bedforms in the miniature braided system are often obliterated in the dry ephemeral channel between flow events, giving rise to clockwise hysteretic bedload response due to bar reformation and the reorganization of the bed surface.
5. The sediment texture of the channel presents differences as large as one order of magnitude between the anabranch subsurface and the bar surface. Bedload texture is thought to vary depending on the topography of the bed. The GSD of the entire sampled bedload is similar to that of the bulk channel subsurface, implying that, on average, bedload transport is generally of equal mobility also when the segregated and unstable bar surfaces are mobile.
6. Measuring bedload in steep channels is a challenge also when the texture is sandy, as it develops a braided pattern. For future studies, it is recommended to accompany the monitoring of bedload with spatially distributed channel change data and simultaneous and accurate water discharge measurements to calculate hydraulic parameters such as stream power, average and local shear stress, thereby furthering our understanding of relevant morphodynamic processes and comparing them to those in other studied braided rivers.

Acknowledgements

This study was funded by Research Projects CGL-2006-07207 and CGL2010-21754-C02-01 of the Spanish Ministry of Science and Technology. Ana Lucía received benefit from a pre-doctoral fellowship funded by the Complutense University of Madrid and Jonathan Laronne participated through a Complutense University Exchange Program. The German Federal Ministry of Education and Research (BMBF) funded the SUMAR project, allowing YSP to participate in this study. The authors acknowledge the kind collaboration of Saturnino de Alba for detrending the slope of the TLS data; Víctor and Toño Muñoz, Cristina Martín-Moreno, Miguel Ángel Sanz-Santos, Ignacio Zapico, and Agustín Blanco for their help in field work, Walter Bertoldi for assistance in the computation of bedload using his formula for braided rivers and Guillermo Pinto in the laboratory. We acknowledge the comments of the editor, Konstantine P. Georgakakos, the associate editor, Luca Mao and two anonymous reviewers; these considerably helped to improve the original manuscript.

References

- Alexandrov, Y., Cohen, H., Laronne, J.B., Reid, I., 2009. Suspended sediment load, bed load, and dissolved load yields from a semiarid drainage basin: a 15-year study. *Water Resour. Res.* 45 (8), W08408.
- Alonso, A., 1981. El cretácico de la provincial de Segovia (borde norte del Sistema Central). *Semin. Estratigr., Ser. Monogr.* 7, 1–271.
- Arcement, G.J., Jr., Schneider, V.R., 1989. Guide for selecting Manning's roughness coefficients for natural channels and flood plains. *Water-Supply Paper*, 2339.
- Ashmore, P.E., 1982. Laboratory modeling of gravel braided stream morphology. *Earth Surf. Process. Landf.* 7, 201–225.
- Ashmore, P.E., 1988. Bed load transport in braided gravel-bed stream models. *Earth Surf. Process. Landf.* 13 (8), 677–695.
- Ashmore, P., 1991. Channel morphology and bed load pulses in braided, gravel-bed streams. *Geogr. Ann., Ser. A, Phys. Geogr.* 73 (1), 37–52.
- Bagnold, R.A., 1966. An approach to the sediment transport problem from general physics. *US Geol. Surv. Prof. Pap.* 422 (1), 37.
- Batalla, R.J., Martín-Vide, J.P., 2001. Thresholds of particle entrainment in a poorly sorted sandy gravel-bed river. *Catena* 44 (3), 223–243.
- Belleudy, P., Valette, A., Graff, B., 2010. Passive hydrophone monitoring of bedload in river beds: first trials of signal spectral analyses. In: Gray, J.R., Laronne, J.B., Marr, J.D.G. (Eds.), *Bedload-surrogate Monitoring Technologies*. *US Geol. Surv. Sci. Investig. Rpt.* 2010-5091, pp. 67–84.
- Bertoldi, W., Ashmore, P., Tubino, M., 2009. A method for estimating the mean bed load flux in braided rivers. *Geomorphology* 103 (3), 330–340.
- Billi, P., 2008. Bedforms and sediment transport processes in the ephemeral streams of Kobo basin, Northern Ethiopia. *Catena* 75 (1), 5–17.
- Billi, P., 2011. Flash flood sediment transport in a steep sand-bed ephemeral stream. *Int. J. Sediment Res.* 26, 193–209.
- Blott, S.J., Pye, K., 2001. GRADISTAT: a grain size distribution and statistics package for the analysis of unconsolidated sediments. *Earth Surf. Process. Landf.* 26, 1237–1248.
- Buckley, S., Howell, J.A., Enge, H.D., Kurz, T.H., 2008. Terrestrial laser scanning in geology: data acquisition, processing and accuracy considerations. *J. Geol. Soc.(Lond.)* 165, 625–638.
- Bunte, K.I., Abt, S.R., Potyondy, J.P., 2001. Portable bedload traps with high sampling intensity for representative sampling of gravel transport in wadable mountain streams. In: *Proc. 7th Interagency Sedimentation Conf., US Subcommittee on Sedimentation*, Reno, Nevada, USA, pp. III-24–III-31.
- Church, M., Jones, D., 1982. Channel bars in gravel-bed rivers. In: Hey, R.D., Bathurst, J.C., Thorne, C.R. (Eds.), *Gravel Bed Rivers*. John Wiley & Sons Ltd., Chichester, pp. 291–338.
- Church, M.A., McLean, D.G., Wolcott, J.F., 1987. River bed gravels: sampling and analysis. In: Thorne, C.R., Bathurst, J.C., Hey, R.D. (Eds.), *Sediment Transport in Gravel-bed Rivers*. John Wiley & Sons, New York, pp. 269–325.
- CNIG (Ed.), 2004. Sección II. Grupo 9. Climatología Atlas nacional de España. Ministerio de Fomento, Madrid.
- Cohen, H., Laronne, J.B., 2005. High rates of sediment transport by flashfloods in the Southern Judean Desert, Israel. *Hydrol. Process.* 19 (8), 1687–1702.
- Cohen, H., Laronne, J.B., Reid, I., 2010. Complex simplicity of bedload response during flash floods in gravel-bed ephemeral rivers: a 10-year field study. *Water Resour. Res.* 46, W11542.

- Cudden, J.R., Hoey, T.B., 2003. The causes of bedload pulses in a gravel channel: the implications of bedload grain-size distributions. *Earth Surf. Process. Landf.* 28 (13), 1411–1428.
- D'Agostino, V., Lenzi, M.A., 1999. Bedload transport in the instrumented catchment of the Rio Cordon: Part II: Analysis of the bedload rate. *Catena* 36 (3), 191–204.
- Dietrich, W.E., Kirchner, J.W., Ikeda, H., Iseya, F., 1989. Sediment supply and the development of the coarse surface layer in gravel-bedded rivers. *Nature* 340, 215–217.
- Du Boys, P., 1879. Étude du régime du Rhône et de l'action exercée par es eaux sur un lit à fond de graviers indéfiniment affouillable. *Annales des Ponts et Chaussées* 18 (5), 141–195.
- Duncan, M.J., Laronne, J.B., 1998. Bedload movement in a wide, gravel bed river: an indication of bar formation. In: Klingeman, P., Beschta, P., Komar, R., Bradley, B. (Eds.), *Gravel-Bed Rivers in the Environment*. Water Resour. Publ. LLC, Highlands Ranch, pp. 741–748.
- Einstein, H., 1950. The bed-load function for sediment transportation in open channel flows. U.S. Department of Agriculture. Technical Bulletin, vol. 1026, p. 71.
- Engelund, F., 1966. Hydraulic resistance of alluvial streams. *J. Hydraul. Div., Amer. Soc. Civil Eng.* 92 (HY 2), 315–326.
- Engelund, F., Hansen, E., 1967. A Monograph on Sediment Transport in Alluvial Streams. Copenhagen, Denmark.
- Ergenzinger, P., Reid, I., Laronne, J.B., Jong, C., 1992. Short term temporal variations in the spatial pattern of bedload transport rate: Squaw Creek, Montana, USA and Nahal Yatir & Eshtemoa, Israel. In: Bogen, J. (Ed.), *Erosion and Sediment Transport Monitoring Programmes in River Basins*. AIHS – IAHS, pp. 77–81.
- Ergenzinger, P., de Jong, C., Laronne, J.B., Reid, I., 1994. Short term temporal variations in bedload transport rates: Squaw Creek, Montana, Usa and Nahal Yatir and Nahal Estemoa, Israel. In: Ergenzinger, P., Schmidt, K.-H. (Eds.), *Dynamics and Geomorphology of Mountain Rivers*. Lecture Notes in Earth Sciences. Institut für Geographische Wissenschaften Frie Universität Berlin, Berlin, pp. 251–264.
- Ferguson, R.I., 2003. The missing dimension: Effects of lateral variation on 1-D calculations of fluvial bedload transport. *Geomorphology* 56, 1–14. [http://dx.doi.org/10.1016/S0169-555X\(03\)00042-4](http://dx.doi.org/10.1016/S0169-555X(03)00042-4).
- Frey, P., Church, M., 2012. Gravel Transport in Granular Perspective. In: Church, M., Biron, P.M., Roy, A.G. (Eds.), *Gravel-Bed Rivers: Processes, Tools, Environments*. John Wiley & Sons, Ltd, pp. 37–55.
- Gaeuman, D., 2010. Mechanics of bedload rating curve shifts and bedload hysteresis in the Trinity River, California. In: 2nd Joint Federal Interagency Conference, Las Vegas, NV, USA.
- Gaeuman, D., Jacobson, R.B., 2006a. Acoustic Bed Velocity and Bed Load Dynamics in A Large Sand Bed River, vol. 111(F2).
- Gaeuman, D., Jacobson, R.B., 2006b. Acoustic bed velocity and bed load dynamics in a large sand bed river. *J. Geophys. Res.* 111 (F02005), 14.
- García, C., Laronne, J.B., Sala, M., 2000. Continuous monitoring of bedload flux in a mountain gravel-bed river. *Geomorphology* 34, 23–31.
- Gaweesh, M.T.K., Van Rijn, L.C., 1994. Bed-load sampling in sand bed rivers. *J. Hydraul. Eng. Amer. Soc. Civil Eng.* 120 (12), 1364–1384.
- Gomez, B., 1983. Temporal variations in bedload transport rates – the effect of progressive bed armouring. *Earth Surf. Process. Landf.* 8 (1), 41–54.
- Gomez, B., 1984. Typology of segregated (armoured/paved) surfaces: some comments. *Earth Surf. Process. Landf.* 9 (1), 19–24.
- Gomez, B., Church, M., 1989. An assessment of bedload sediment transport formulae for gravel bed rivers. *Water Resources Res.* 25, 1161–1186. <http://dx.doi.org/10.1029/WR025i006p01161>.
- Gomez, B., Naff, R.L., Hubbell, D.W., 1989. Temporal variations in bedload transport rates associated with the migration of bedforms. *Earth Surf. Process. Landf.* 14 (2), 135–156.
- Good, T.R., Bryant, I.D., 1985. Fluvio-aeolian sedimentation: an example from Banks Island, N.W.T., Canada. *Geogr. Ann., Ser. A, Phys. Geogr.* 67 (1/2), 33–46.
- Gray, J.R., Laronne, J.B., Marr, J.D.G., 2010. Bedload-surrogate Monitoring Technologies, 2010-5091, p. 37.
- Habersack, H., Nachtnebel, P.N., Laronne, J.B., 2001. The continuous measurement of bedload discharge in a large alpine gravel bed river. *J. Hydraul. Res.* 39 (2), 125–133.
- Haff, P.K., 1996. Limitations of predictive modeling in geomorphology. In: Rhoads, B.L., Thorn, C.E. (Eds.), *The Scientific Nature of Geomorphology*. John Wiley & Sons, pp. 337–358.
- Hassan, M.A. et al., 2005. Sediment transport and channel morphology of small forested streams. *J. Am. Water Resour. Assoc.* 41, 853–876.
- Hassan, M.A., Egozi, R., Parker, G., 2006. Experiments on the effect of hydrograph characteristics on vertical grain sorting in gravel bed rivers. *Water Resour. Res.* 42 (9).
- Hayes, S.K., Montgomery, D.R., Newhall, C.G., 2002. Fluvial sediment transport and deposition following the 1991 eruption of Mount Pinatubo. *Geomorphology* 45 (3–4), 211–224.
- Helley, E.J., Smith, W., 1971. Development and calibration of a pressure-difference bed load sampler. U.S. Geol. Surv. Open File Report, Washington, DC, USA, 18 pp.
- Hoey, T.B., Sutherland, A.J., 1991. Channel morphology and bedload pulses in braided rivers: a laboratory study. *Earth Surf. Process. Landf.* 16 (5), 447–462.
- Holmes, R.R.J., 2010. Measurement of bedload transport in sand-bed rivers: a look at two indirect sampling methods. In: Gray, J.R., Laronne, J.B., Marr, J.D.G. (Eds.), *Bedload-surrogate Monitoring Technologies*. U.S. Geol. Surv. Sci. Investig. Rpt. 2010-5091.
- Humphries, R., Venditti, J.G., Sklar, L.S., Wooster, J.K., 2012. Experimental evidence for the effect of hydrographs on sediment pulse dynamics in gravel-bedded rivers. *Water Resour. Res.* 48 (1), 1–15.
- Iseya, F., Ikeda, H., 1987. Pulsation in bedload transport rates induced by a longitudinal sediment sorting. A flume study using sand and gravel mixtures, *Geografiska Annaler*. vol. 69(A), pp. 15–27.
- Lancaster, S.T., Grant, G.E., 2003. You want me to predict what? In: Wilcock, P.R., Iverson, R.M. (Eds.), *Prediction in Geomorphology*. Geophysical Monograph 135. American Geophysical Union, pp. 1–10.
- Laronne, J.B., Reid, I., 1993. Very high rates of bedload sediment transport by ephemeral desert rivers. *Nature* 366, pp. 148–150.
- Laronne, J.B., Reid, I., Yitshak, Y., Frostick, L.E., 1994. The non-layering of gravel streambeds under ephemeral flood regimes. *J. Hydrol.* 159 (1–4), 353–363.
- Laronne, J.B., et al., 2003. The continuous monitoring of bedload flux in various fluvial environments. In: Bogen, J., Fregus, T., Walling, D.E. (Eds.), *Erosion and Sediment Transport Measurement in Rivers: Technological and Methodological Advances*. Int'l Assoc. Hydrol. Sci. Publ., pp. 134–145.
- Leopold, L.B., 1994. A View of The River. Harvard University Press, Cambridge, Massachusetts, 298 pp..
- Leopold, L.B., Emmett, W.W., 1977. Bedload measurements, East Fork River, Wyoming. Wyoming. Proc. Natl. Acad. Sci. USA 74, 2644–2648.
- Leopold, L.B., Wolman, M.G., Miller, J.P., 1964. Fluvial processes in geomorphology. Books in Geology. W.H. Freeman and Company, San Francisco.
- Lucía, A., Laronne, J.B., Martín-Duque, J.F., 2011. Geodynamic processes on sandy slope gullies in central Spain – field observations, methods and measurements in a singular system. *Geodin. Acta* 24 (2), 61–79.
- Mao, L., 2012. The effect of hydrographs on bed load transport and bed sediment spatial arrangement. *J. Geophys. Res.* 117 (F3), F03024.
- Mao, L., Comiti, F., Lenzi, M.A., 2010. Bedload dynamics in steep mountain rivers: insights from the Rio Cordon experimental station (Italian Alps). In: Gray, J.R., Laronne, J.B., Marr, J.D.G. (Eds.), *Bedload-surrogate Monitoring Technologies*. U.S. Geol. Surv. Sci. Investig. Rpt. 2010-5091, pp. 253–265.
- Meyer-Peter, E., Müller, R., 1948. Formulas for Bed-load Transport. In: 2nd Meeting, IAHR. IAHR, Stockholm, Sweden, pp. 39–64.
- Milhou, R.T., 1973. Sediment transport in a gravel-bottomed stream. Unpublished PhD Thesis, Oregon State University, Corvallis, 232 pp.
- Mizuyama, T., et al., 2010. Calibration of a passive acoustic bedload monitoring system in Japanese mountain rivers. In: Gray, J.R., Laronne, J.B., Marr, J.D.G. (Eds.), *Bedload-surrogate Monitoring Technologies*. U.S. Geol. Surv. Sci. Investig. Rpt. 2010-5091, pp. 296–318.
- Nelson, P.A., Venditti, J.G., Dietrich, W.E., Kirchner, J.W., Ikeda, H., Iseya, F., Sklar, L.S., 2009. Response of bed surface patchiness to reductions in sediment supply. *J. Geophys. Res.* 114, F02005. <http://dx.doi.org/10.1029/2008JF001144>.
- Nicholas, A.P., 2000. Modelling bedload yield in braided gravel bed rivers. *Geomorphology* 36 (1–2), 89–106.
- Paola, C., 1996. Incoherent structure: turbulence as a metaphor for stream braiding. p. 705-723 in P. J. Ashworth, Bennett, S.J., Best, J.L., McLelland, S. (eds.): *Coherent Flow Structures in Open Channels*. John Wiley & Sons, Chichester.
- Parker, G., 2008. Transport of gravel and sediment mixtures. In: García, M.H. (Ed.), *Sedimentation Engineering: Processes, Measurements, Modeling, and Practice*. Manual and Reports on Engineering Practice. ASCE, Reston, Virginia, pp. 165–252.
- Poreh, M., Sagiv, A., Seginer, I., 1970. Sediment sampling efficiency of slots. *J. Hydraul. Eng.* 96, 2065–2078.
- Powell, D.M., Reid, I., Laronne, J.B., 1999. Hydraulic interpretation of cross-stream variations in bed-load transport. *J. Hydraul. Eng. Amer. Soc. Civil Eng.* 125 (12), 1243–1252.
- Powell, D.M., Reid, I., Laronne, J.B., 2001. Evolution of bed load grain size distribution with increasing flow strength and the effect of flow duration on the caliber of bed load sediment yield in ephemeral gravel bed rivers. *Water Resour. Res.* 37 (5), 1463–1474.
- Powell, D.M., Laronne, J.B., Reid, I., 2003. The dynamics of bedload sediment transport in low-order, upland, ephemeral gravel-bed rivers. *Adv. Environ. Monit. Model.* 1 (2), 1–27.
- Powell, D.M., Laronne, J.B., Reid, I., Barzilai, R., 2012. The bed morphology of upland single-thread channels in semi-arid environments: evidence of repeating bedforms and their wider implications for gravel-bed rivers. *Earth Surf. Process. Landf.* 37 (7), 741–753.
- Recking, A., Frey, P., Paquier, A., Belleudy, P., 2009. An experimental investigation of mechanisms involved in bed load sheet production and migration. *J. Geophys. Res.* 114, 13.
- Recking, A., 2010. A comparison between flume and field bed load transport data and consequences for surface based bed load transport prediction. *Water Resources Res.* 46. <http://dx.doi.org/10.1029/2009WR008007>.
- Reid, I., Layman, J.T., Frostick, L.E., 1980. The continuous measurement of bedload discharge. *J. Hydraul. Res.* 18 (3), 243–249.
- Reid, I., Powell, D.M., Laronne, J.B., 1996. Prediction of bed-load transport by desert flash floods. *J. Hydraul. Eng.* 122 (3), 170–173.
- Reid, I., Laronne, J.B., Powell, D.M., 1998. Flash-flood and bedload dynamics of desert gravel-bed streams. *Hydrol. Process.* 12, 543–557.
- Rennie, C.D., Villard, P.V., 2004. Site specificity of bedload measurement using an ADCP. *J. Geophys. Res.* 109 (F3), F03003.
- Rice, S.P., Church, M., 2010. Grain-size sorting within river bars in relation to downstream fining along a wandering channel. *Sedimentology* 57 (1), 232–251.

- Rice, S.P., Church, M., Wooldridge, C.L., Hickin, E.J., 2009. Morphology and evolution of bars in a wandering gravel-bed river; lower Fraser river, British Columbia, Canada. *Sedimentology* 56 (3), 709–736.
- Rickenmann, D., Fritschi, B., 2010. Bedload transport measurements using piezoelectric impact sensors and geophones. In: Gray, J.R., Laronne, J.B., Marr, J.D.G. (Eds), *Bedload-surrogate Monitoring Technologies*. U.S. Geol. Surv. Sci. Investig. Rpt. 2010-5091, pp. 407–423.
- Rickenmann, D., McArdell, B.W., 2007. Continuous measurement of sediment transport in the Erlenbach stream using piezoelectric bedload impact sensors. *Earth Surf. Process. Landf.* 32, 1362–1378.
- Schaank, E.M.H., 1937. Discussion d Smetana, J.: Appareil pour le jaugeage du débit solide entraîné sur le fond du cours d'eau. In: 1st Meet. Int. Ass. Hydraul. Struct. Res. Append, pp. 93–120.
- Smart, G., Jaeggi, M., 1983. Sediment transport on steep slopes. *Mitteilungen der Versuchsanstalt für Wasserbau, Hydrologie und Glaziologie*, vol. 64, Zurich, pp. 91–191.
- Turowski, J.M., 2010. Probability distributions of bed load transport rates: a new derivation and comparison with field data. *Water Resour. Res.*, 46.
- Van Rijn, L., 1984. Sediment Transport, Part I: Bed Load Transport. *J. Hydraul. Eng.* 110 (10), 1431–1456.
- Van Rijn, L.C., Gaweesh, M., 1992. A new total load sampler. *J. Hydraul. Eng.* 118 (12).
- Vericat, D., Batalla, R.J., 2010. Sediment transport from continuous monitoring in a perennial Mediterranean stream. *Catena* 82 (2), 77–86.
- Whitaker, A.C., Potts, D.F., 2007. Analysis of flow competence in an alluvial gravel bed stream, Dupuyer Creek. *Montana. Water Resour. Res.* 43 (7), W07433.
- Whiting, P.J., Dietrich, W.E., Leopold, L.B., Drake, T.G., Shreve, R.L., 1988. Bedforms in heterogeneous sediment. *Geology* 16 (2), 105–108.
- Williams, G.P., 1989. Sediment concentration versus water discharge during single hydrologic events in rivers. *J. Hydrol.* 111, 89–106.